TISSUE ENGINEERING
Volume 5, Number 3, 1999
Mary Ann Liebert, Inc.

Autologous Mesenchymal Stem Cell-Mediated Repair of Tendon

HANI A. AWAD, Ph.D.,[1] DAVID L. BUTLER, Ph.D.,[1]
GREGORY P. BOIVIN, D.V.M., M.S.,[2] FROST N.L. SMITH, M.S.,[2]
PRASANNA MALAVIYA, Ph.D.,[3] BARBARA HUIBREGTSE, D.V.M.,[4] and
ARNOLD I. CAPLAN, Ph.D.[5]

ABSTRACT

Mesenchymal stem cells (MSCs) were isolated from bone marrow of 18 adult New Zealand White rabbits. These cells were culture expanded, suspended in type I collagen gel, and implanted into a surgically induced defect in the donor's right patellar tendon. A cell-free collagen gel was implanted into an identical control defect in the left patellar tendon. Repair tissues were evaluated biomechanically ($n = 13$) and histomorphometrically ($n = 5$) at 4 weeks after surgery. Compared to their matched controls, the MSC-mediated repair tissue demonstrated significant increases of 26% ($p < 0.001$), 18% ($p < 0.01$), and 33% ($p < 0.02$) in maximum stress, modulus, and strain energy density, respectively. Qualitatively, there appeared to be minor improvements in the histological appearance of some of the MSC-mediated repairs, including increased number of tenocytes and larger and more mature-looking collagen fiber bundles. Morphometrically, however, there were no significant left-right differences in nuclear aspect ratio (shape) or nuclear alignment (orientation). Therefore, delivering a large number of mesenchymal stem cells to a wound site can significantly improve its biomechanical properties by only 4 weeks but produce no visible improvement in its microstructure.

INTRODUCTION

MESENCHYMAL PROGENITOR OR STEM CELLS are becoming a subject of increasing interest because of their potential utility in tissue engineering applications. By definition, stem cells not only can self-renew through repeated mitotic divisions, but also can differentiate along various, specialized lineages.[1,2] Progenitor cells (often called mesenchymal stem cells or MSCs) give rise to the body's skeletal cells during embryonic development.[1] MSCs reside in the marrow in long bone cavities and in the periosteal shell of long

[1]Noyes-Giannestras Biomechanics Laboratories, Department of Aerospace Engineering and Engineering Mechanics, and [2]Department of Laboratory Medicine, Division of Comparative Pathology, University of Cincinnati, Cincinnati, Ohio.

[3]Institute of Bioengineering and Bioscience, Georgia Institute of Technology, Atlanta, Georgia.

[4]Genzyme Tissue Repair, Inc., Boston, Massachusetts.

[5]Skeletal Research Center/Department of Biology, Case Western Reserve University, Cleveland, Ohio.

bone.[1,3,4] Throughout life, MSCs continue to provide specialized progeny of cells that are involved in homeostatic remodeling of the skeletal system and repair of injured tissue.[3,5]

Previous studies have shown evidence for the potential applications of MSCs. For example, demineralized bone matrix has been shown to stimulate the differentiation of cartilage and bone from MSCs located in the connective tissue or stroma of several organs.[6,7] Caplan et al.[8] found that MSCs isolated from marrow have the potential to form cartilage and bone when incorporated into porous ceramic cubes and implanted into subcutaneous sites *in vivo*. Furthermore, orthopedic surgeons have long appreciated that factors such as vascular continuity, excess marrow, and intact periosteum may correlate with accelerated long bone repair.[9] It is quite possible that MSCs in marrow and periosteum, in addition to other factors such as growth factors and cytokines that are delivered to the fracture site through the blood supply, might function to accelerate repair. The exact mechanisms by which these factors act in synergy is yet to be uncovered.

The concept of recruiting MSCs to accelerate repair and tissue regeneration has been tested *in vivo* in cartilage,[10] in bone,[11,12] and more recently in the Achilles tendon.[13,14] These studies have demonstrated various degrees of improvement in the repair outcome, indicating the merits of MSCs as a potential therapy, but at the same time, suggesting the need for more basic science research before clinical utility can become a possibility. Therefore, the current study was designed to test the hypothesis that MSCs, when culture-expanded, seeded in collagen gel and then implanted *in vivo*, will help improve the biomechanical properties and structural organization of repair tissues of window defects surgically induced in the rabbit patellar tendon.

METHODS

Animal Model

Eighteen 12-month old, Pasteurella-free, female New Zealand White rabbits, weighing 3.0 to 5.0 kg, were acquired (Covance Research Products, Denver, PA), and acclimated for at least 1 week before surgery in individual cages. Subsequently, each rabbit received bilateral implant surgery and was assigned for either biomechanical evaluation ($n = 13$) or histomorphometric analysis ($n = 5$) 4 weeks after the surgical procedure. Use of animals was conducted in accordance with protocols approved by the Institutional Animal Care and Use Committee at Children's Hospital Research Foundation (Cincinnati, OH).

Marrow Harvest, MSC Isolation, and Culture

Under general anesthesia and aseptic conditions, bone marrow was collected from the rabbit's iliac crest using a 16-gauge needle, connected to an extension tube fastened to a 10-cc syringe. All components of the collection system were charged with 1 ml (3,000 U/ml) of sodium heparin (Elkins-Sinn, Inc., Cherry Hill, NJ) to prevent coagulation. The marrow was suspended in 50 ml Falcon® (Becton Dickinson Labware, Franklin Lakes, NJ) tubes using 10 ml of Dulbecco's modified Eagle's medium containing low glucose (DMEM-LG) supplemented with screened lots[15] of 10% fetal bovine serum (FBS) (Intergen, Purchase, NY). Tubes were sealed with parafilm, and shipped overnight on ice packs (−4°C) to the coauthors' laboratory (B.H., A.I.C.) in Cleveland.

Marrow samples were centrifuged at 1500*g* for 5 minutes. The supernatant was discarded and the cells were resuspended in DMEM-LG supplemented with 10% FBS (complete medium). A small aliquot of cells was diluted 1:7 with 2 parts of 4% acetic acid to disrupt the red blood cells and 5 parts serum-free DMEM-LG to facilitate cell counting in a hemacytometer (Fisher Scientific, Pittsburgh, PA). After appropriate final dilution in complete medium, the cells were seeded onto 100 mm Falcon® dishes (20 million cells in 7 ml) as previously described.[10] Complete medium was changed after 4 days in culture and every 3 to 4 days thereafter. Cells were kept in primary culture for 14 days until 85% confluent, at which time cells were released from the dishes by exposure to 0.05% trypsin in EDTA (Sigma Chemical, St. Louis, MO) and seeded into 75 cm^2 flasks at a concentration of 1 million cells per flask. Once the cells approached 85% confluency, the flasks were filled with complete media, sealed with parafilm, and returned on ice packs overnight to Cincinnati.

Preparation of MSC Implants

Once received, the MSCs were released from the culture flasks and collected by centrifugation. Cells were then suspended at a final concentration of 5×10^6 cells/ml in a 1:1 mixture of DMEM and 0.3% acid-soluble type-I bovine collagen solution (Pancogene-S®, Gattefossé, Lyon, France), as previously described.[10] Based upon *in vitro* data, we determined that there were no significant differences in contraction kinetics or maximum contraction for collagen gels seeded with 4×10^6 and 8×10^6 cells/ml.[16] Therefore, we selected a concentration of 5×10^6 cells/ml to ensure maximum contraction *in vitro* prior to implantation. The resulting cell suspension was then carefully pipetted into a sterile, hemispherical trough (I.D. of 8 mm) placed inside a 100-mm sterile Falcon® dish. The dish was incubated at 37°C in a humidified chamber of 5% carbon dioxide for an initial period of 30 min to allow the mixture (hereafter the MSC implant) to set, after which the dish was flooded with serum-free medium and placed back in the incubator overnight. Eighteen hours after implant preparation, the implant had contracted to about 50% of its initial size, which was large enough to completely fill the surgical defect. A cell-free collagen gel implant for the contralateral control patellar tendon defect was similarly prepared by mixing serum-free medium with type I collagen solution in equal proportions.

Surgical Procedure

The rabbit was anesthetized with an intramuscular injection of a mixture of 40 mg/kg of ketamine hydrochloride (Ketaset; Fort Dodge Laboratories, Fort Dodge, IA) and 5 mg/kg of xylazine (Rompun; Miles, Shawnee Mission, KS). Both knees were shaved and prepped with an iodine scrub solution and alcohol. Both patellar tendons (PTs) were exposed through 6–8 cm longitudinal incisions. Identical, full-thickness, window defects were cut in the central part of each patellar tendon. The corners of each defect were marked with blue monofilament polypropylene suture (5-0 Prolene, Ethicon, Inc., Somerville, NJ) to help identify the wound site at the time of sacrifice and dissection. The initial medial and lateral length (3.8 ± 0.5mm long), and proximal and distal width (3.8 ± 0.6 mm wide) were then recorded. The right PT defect was then grafted with the autologous MSC implant. The implant was secured in place with the knee at 90° flexion. A biodegradable suture (5-0 Dexon, Davis & Geck, Inc., Manati, PR) was passed through the implant and secured under tension to the proximal and distal edges of the defect. The epitenon was then closed over the defect to cover and maintain the MSC implant. The skin was then closed with interrupted sutures. The left PT defect was filled with the cell-free collagen implant and a biodegradable suture, similar to the treated side.

Biomechanical Evaluation

Each rabbit was killed with an intracardiac injection of sodium pentobarbital (100 mg/kg) at 4 weeks postimplantation. PTs assigned for biomechanical testing were harvested with bone blocks at both ends. PT dimensions were recorded. The frontal repair area was identified using the corner-marking sutures and the length and width were measured. Each bone end was fixed in polymethylmethacrylate (Dentsply® Repair Material, Dentsply International, Inc., York, PA) embedded in special PT grips. Tissue struts lateral and medial to the defect region were removed, and the length and thickness of the remaining repair tissue were measured at three locations (proximal and distal edges, and center) using vernier calipers, and then averaged. Each specimen was mounted on a testing system (Model 8501, Instron Corp., Canton, MA) in a bath of Dulbecco's phosphate-buffered saline at 37°C and a pH of 7.5 ± 0.3 (Sigma Chemical, St. Louis, MO). Each repair tissue was failed in tension under displacement control at a slow strain rate (2% per second), while automatically recording the Instron load cell force and actuator displacement data. The force-elongation data were then used to determine the structural properties of the repair tissue: stiffness, maximum force, and energy to maximum force.[17–20] The corresponding material properties: modulus, maximum stress, and strain energy density to maximum stress were also calculated by adjusting for initial tissue length and repair area.[20] The failure tests were videotaped using a video camcorder (RCA Model CC415, Thomson Electronics, Inc., Indianapolis, IN) and played back to verify the failure sequence in each test.

Histology and Morphometry

PTs for histology and morphometric analysis were freshly harvested after sacrifice, fixed in 10% neutral buffered formalin at room temperature for 24 h, and then dehydrated through a gradient of alcohols for paraffin embedding. Five-micron thick serial sections were cut in the coronal plane and then stained with hematoxylin and eosin, Harris hematoxylin (for gray scale morphometric image analysis), and Gomori's Trichrome for collagen staining.

Sections were examined under 1-40× magnification (Model BH-2, Olympus Optical Co., Tokyo, Japan) to assess infiltration of inflammatory cells and fibroblasts and to examine gross matrix and cellular organization and vascularity of the repair site. Images of sections for semiautomated morphometric analysis were transferred to a Macintosh computer (Model Quadra 950, Apple Computer, Inc., Cupertino, CA). Morphometric analysis of each section was performed at 14 view fields within six regions (Figure 1). These regions included four sites within the repair area (R); two sites at each of regions proximal (P), distal (D), medial (M), and lateral (L) to the repair region; and two normal fields (N) remote from the repair site (not shown in Figure 1). NIH Image 1.60 program was used to quantify cellular morphometric features. These measurements included cell number density (defined as the cell number per unit area), nuclear aspect ratio (minor/major nuclear axis dimension), and nuclear alignment angle (with respect to the long axis of the tendon). This alignment angle was quantified between ± 90° in 10° bands. The fraction of nuclei within each angular band, x, was calculated. An entropy parameter, H, indicative of random disorganization in nuclear alignment, was also determined as previously described by Frank et al[21]:

$$H = -\sum_{i=1}^{18} x_i \log_2 x_i$$

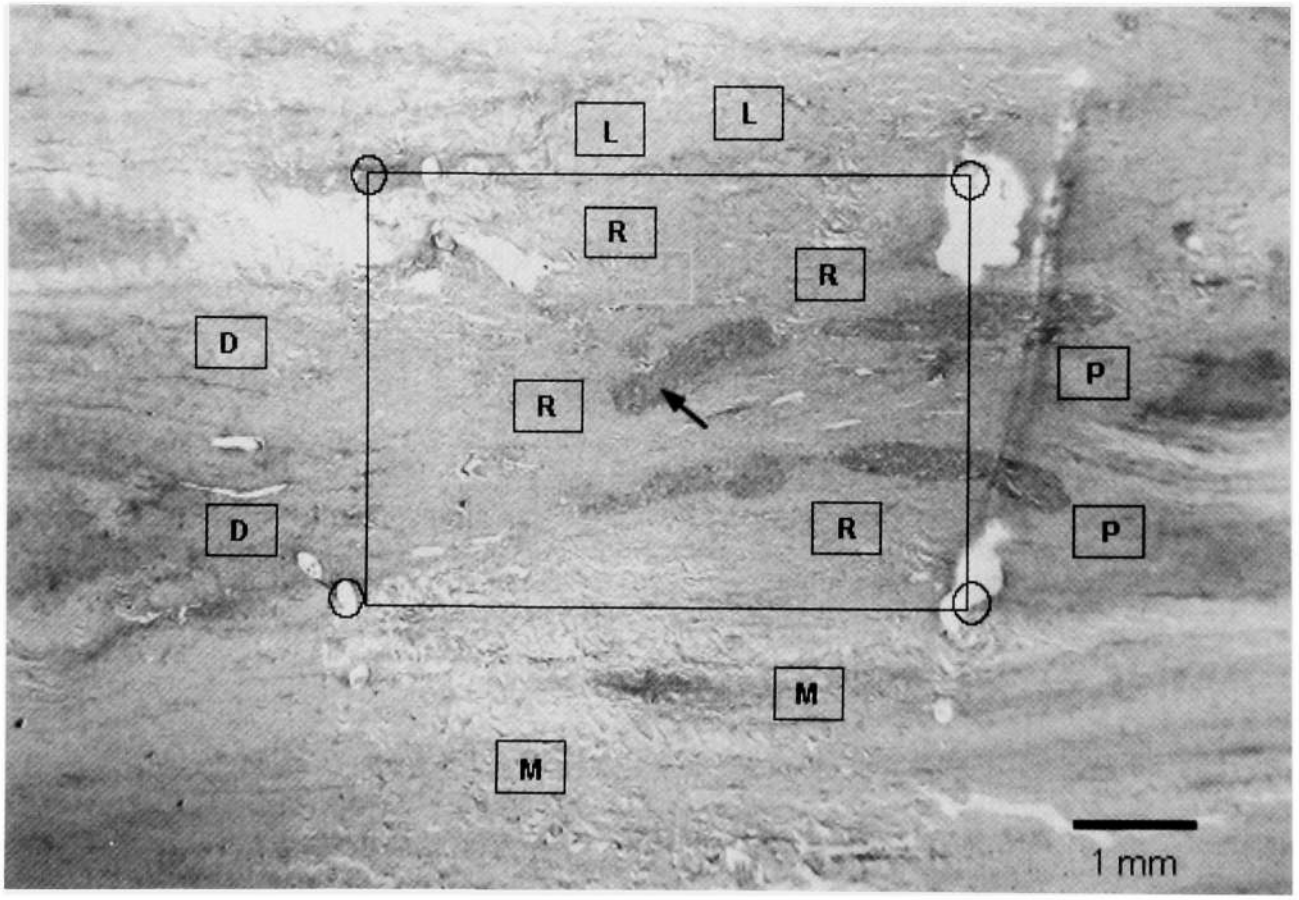

FIG. 1. Morphometric analysis regions in the healing rabbit patellar tendons: (R) repair site, (P) proximal region, (D) distal region, (M) medial region, (L) lateral region. The circles are placed at the holes left by the marking suture at the corners of the original defect. Normal regions (N) were regions far away from the repair site that do not appear in this frame (1×). The arrow points toward the residues of the biodegradable suture.

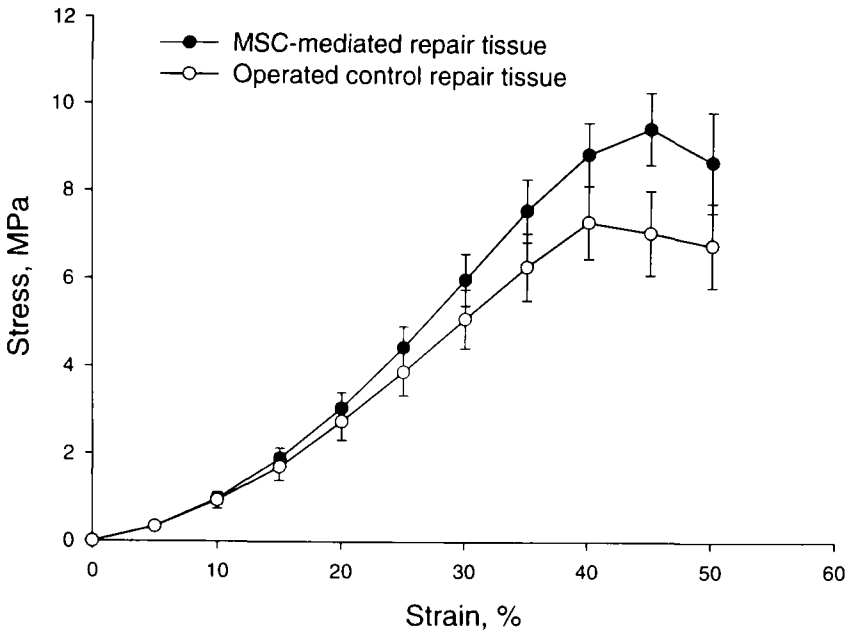

FIG. 2. Average stress-strain curves for rabbit patellar tendon repair tissues at 4 weeks after injury and repair (error bars correspond to SEM).

Entropy defines a score of the randomness of nuclear orientation where lower entropy values signify better alignment of nuclei.

Statistical Analysis

Paired-difference *t*-tests were performed to test the significance of the treatment effects on the biomechanical properties, entropy parameters, and cell density. Differences were accepted as significant when the type I error probability (α) did not exceed 0.05. The morphometric data (nuclear aspect ratio and nuclear orientation) were tested using nonparametric (distribution-free) methods because our nuclear measurements were found to deviate from the normal distribution. The Kolmogorov-Smirnov test was utilized to test for differences in the distributions of the nuclear aspect ratio and orientation for the treated and control samples ($\alpha = 0.05$).[22]

RESULTS

No significant left-right differences were found between the frontal area of the repair site, either at the time of surgery (15.0 ± 3.5 versus 14.0 ± 2.0 mm^2 $p = 0.24$) or at 4 weeks postsurgery (32.7 ± 31.2 versus 31.7 ± 27.2 mm^2, $p = 0.75$). However, after 4 weeks, the lesions had elongated and widened such that the final frontal repair areas were significantly larger than the initial repair areas for both sides ($p < 0.05$). The cross-sectional areas of the treated repair tissues (12.4 ± 3.9 mm^2) were not statistically different than the areas for the contralateral controls (11.9 ± 5.1 mm^2, $p = 0.37$).

The biomechanical properties of the treated repair tissues showed significant improvements compared to their contralateral controls (Figure 2). The modulus in the linear region for the MSC-treated tissues was approximately 18% greater than the value for the contralateral controls ($p < 0.01$; Table 1). The maximum stress and strain energy density for the treated repair tissues were nearly 26% ($p < 0.05$) and 33% ($p < 0.005$) greater, respectively, than values for their matched controls. There were no significant differences in the strain at maximum stress between the treated and control repair tissues, however (Table 1). Stiffness, maximum force, and energy to maximum force for the MSC repairs were approximately 15, 28, and 40% greater than their paired controls, respectively. The maximum elongation (i.e., elongation at maximum force)

for the treated repair tissues was not significantly different from that for the operated controls (Table 1). As verified by the video records, all the specimens tested exhibited midsubstance (soft tissue) failures.

Histologic analysis revealed no consistent differences between treated and operated-control repairs. In two tendon pairs, the MSC-treated lesions showed a more organized and mature structure than for controls. This structure was characterized by better alignment of cells, as well as thicker and more crimped collagen fibers that were often indistinguishable from the surrounding, normal collagen (Figure 3). The three remaining pairs of tendons showed good-to-excellent alignment of tenocytes within the wound site, but with no detectable differences between the treated and control lesions. In most of the tendons, groups of fibroblasts extended both proximally and distally from the wound site, with more normal tenocytes sandwiched in between these cell tracks. These fibroblasts were generally associated with thinner collagen fibers that stained only lightly for eosin. Neutrophil and lymphocyte inflammatory infiltration was localized around the biodegradable sutures or new vessels in the wound site.

Morphometry defined important features of this repair model. The treated repair sites exhibited similar cell densities (2268 ± 493 cells/mm^2) compared to their paired controls (2093 ± 493 cells/mm^2, $p = 0.22$). In general, regional variations in cell density in both treated and control tendons were similar (Table 2). The regions proximal and distal to the repair site were approximately 35–45% more densely populated with cells compared to the regions medial and lateral to the repair site ($p < 0.05$). These medial and lateral regions, in turn, contained almost twice the cell density of the normal regions, N, ($p < 0.0001$). Nuclei in the repair regions and in the regions proximal and distal to the repair were also more rounded than nuclei medial and lateral to the repair as manifested by the significantly higher nuclear aspect ratios ($p < 0.005$, Table 2). Cells in remote normal regions, N, displayed nuclear aspect ratios that were significantly lower than in all other regions ($p < 0.005$, Table 2). Entropy was not significantly different in regions R, P, D, M, and L between and across all treated and control tendons ($p > 0.05$). However, in all tissues, the entropy was significantly lower in the normal regions compared to all other regions ($p < 0.05$, Table 2).

DISCUSSION

The findings from this study support our hypothesis that MSCs, when implanted into tendon defects, provide significantly greater material and structural properties compared to repairs containing only collagen gel alone. We demonstrated significant, 15–40% increases in structural properties due to the presence of MSCs. While it could be argued that such increases might be attributed to simply more repair tissue on the treated side (*i.e.*, a larger cross-sectional area), even the material properties of the MSC-treated repairs,

Table 1. Structural and Material Properties for Treated and Control Repair Tissues

	MSC-treated repairs[†]	*Operated control repairs*	*Significance*[‡]
Stiffness, *N/mm*	59.9 (20.6)[§]	51.9 (20.4)	$.05 < p < .06$
Maximum force, *N*	139.1 (55.2)	108.2 (51.1)	$p < .05$
Strain energy, *N/mm*	212.4 (99.6)	151.3 (107.7)	$.05 < p < .06$
Maximum elongation, *mm*	3.17 (0.97)	3.19 (1.17)	$p < 0.47$
Modulus, *MPa*	31.7 (8.9)	26.8 (5.8)	$p < .01$
Maximum stress, *MPa*	11.5 (3.3)	9.1 (3.2)	$p < .005$
Strain energy density, *N.mm/mm^3*	2.8 (1.5)	2.1 (0.9)	$p < .02$
Maximum strain, *%*	15.3 (3.1)	15.1 (3.2)	$p = 0.47$

[§]Mean (standard deviation).

[†]$n = 13$.

[‡]Structural properties (stiffness, maximum force, strain energy, and maximum elongation), and material (modulus, maximum stress, strain energy density, and strain) for both treated and control repair tissues were contrasted using paired difference *t*-tests.

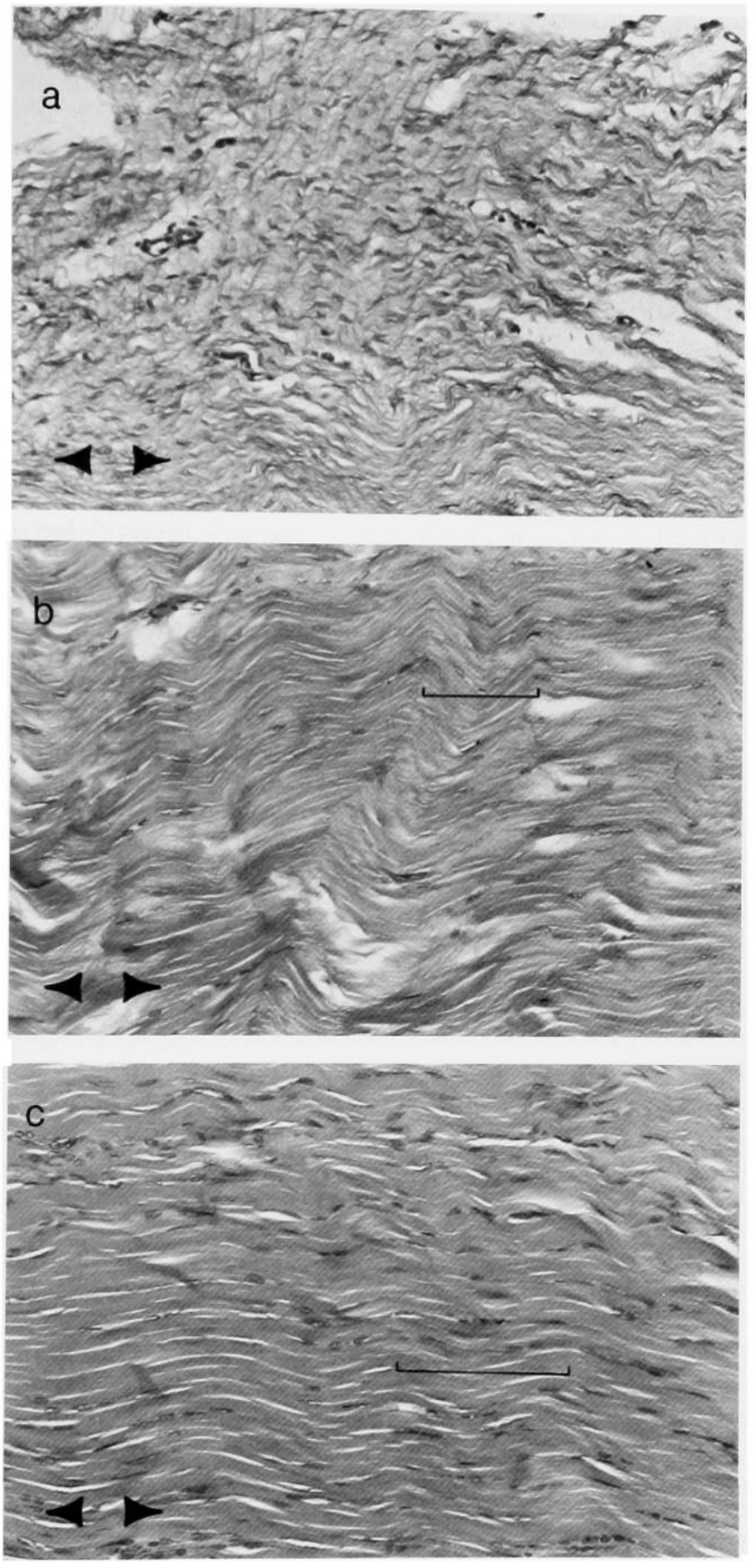

FIG. 3. Typical histologic appearance of (**a**) cell-free implant repair region, (**b**) MSC-treated repair region, and (**c**) normal patellar tendon at 4 weeks postsurgery. Arrows indicate the axial direction of the tendon. Brackets in (b) and (c) indicate length of typical crimp periods. Hematoxylin and eosin staining (20×).

TABLE 2. AVERAGE REGIONAL MORPHOMETRIC PARAMETERS OF THE HEALING RABBIT PATELLAR TENDON

	Cell number density cells/mm²		*Nuclear aspect ratio*		*Nuclear entropy*	
	Treated	*Control*	*Treated*	*Control*	*Treated*	*Control*
Repair region (R)	2268 (493)[§]	2093 (239)	0.448 (0.06)[c]	0.421 (0.02)	3.46 (0.31)[d]	3.22 (0.28)
Proximal & distal regions (P&D)	2179 (353)[a]	2142 (387)	0.421 (0.05)	0.409 (0.041)	3.24 (0.41)	3.24 (0.44)
Medial & lateral regions (M&L)	1498 (387)[a,b]	1583 (633)	0.378 (0.04)	0.376 (0.054)	3.22 (0.36)	3.01 (0.33)
Normal regions (N)	726 (261)[a,b]	756 (449)	0.350 (0.03)[c]	0.342 (0.036)	2.83 (0.58)[d]	2.82 (0.39)

[§]Mean (standard deviation) $n = 5$.
[a,b,c,d]$p < 0.05$.

which are independent of tissue dimensions, were 18–33% greater than matched controls. Thus, repair quality as well as structural integrity were enhanced by the use of MSCs.

At the same time, these treatment-related improvements were not impressive when compared to normal tendon. For example, we found that the modulus, maximum stress, and strain energy density for the treated repairs were, respectively, still only 7, 16, and 32% of normal patellar tendons from a similar group of rabbits.[23] These values seem very low compared to the repair outcomes from other published reports for PT at greater than 1 month after surgery.[24,25] For example, Beynnon et al.[24] reported that the maximum force of the rabbit PT dropped to 53% of normal values immediately after removal of its central third. The maximum force of the healing tendon increased to only 54% of normal PT at 4 weeks, 60% at 8 weeks, and 72% at 6 months.[24] Similarly, Burks et al.[25] reported that the maximum force of the canine PT was only 47% of normal values immediately following removal of its central one-third, increasing to about only 61% of normal after 6 months.[25] However, these results represent not only the properties of repair tissue, but also the biomechanics of adjacent normal struts used to protect the repair during healing. The injury models are also more traumatic than our window defects, which further confounds any direct comparisons between our results and theirs.

Unfortunately, our histologic and morphometric observations failed to explain the improvements in repair biomechanics at this early phase of healing. In particular, we saw no consistent left-right differences in tenocyte alignment or collagen fiber maturation. Three explanations might be considered. (1) Attempts to visually distinguish histologic differences in treatment effects are simply not sensitive enough, unless the differences are very large. (2) Four weeks may be too early to discern the greatest differences in repair histology. Longer intervals of healing might elicit such differences. (3) The structure and biomechanics of healing soft tissues may not correlate well, as others have found in rabbit medial collateral ligament.[26,27] Instead, biomechanics may better correlate with biochemical indices such as collagen cross-link density.[26–28] Unfortunately, such biochemical parameters were not measured.

One concern in the initial study design was the choice of a proper matrix material that would ensure effective delivery of the cells to the repair site. We chose a collagen-based matrix, not only because type I collagen is the most abundant protein in tendon extracellular matrix, but because others have also utilized such gels for tendon repair[13] with success. During incubation, the cells caused a contraction of the collagen gel to about 50% of its initial size, resulting in a structure that is compact, and more surgically manageable. Such contraction likely traps the cells in the implant and more effectively delivers them into the repair site. This contraction of the collagen matrix may also induce morphological and cytoskeletal changes to the seeded cells that stimulate new synthesis of extracellular matrix.[29] Unfortunately, we did not characterize the cell morphology or implant shape during incubation of the constructs used in this study. It is, however, conceivable that the contractile ability of the seeded cells may serve as an index and predictor of repair outcome. This question will be addressed in our future research.

The cell-free collagen gel maintained its fluidity and did not contract during incubation. We suspect that these cell-free implants may have leaked outside the defect site but, unfortunately, we had no way

to determine the fate of the gel once the incision was closed. Therefore, we can not state with certainty the fate of all cell-free implants postsurgery. To ensure that the cells remain in the repair site to effect healing, we now use a fluorescent lipophilic cell membrane label (CellTracker™ CM-DiI, Molecular Probes, Inc., Eugene, OR) to tag the cells during incubation. We have recently shown in unpublished studies that labeled cells remained in the defect and did not migrate into adjacent tissue for up to 6 weeks after surgery. These results are part of a larger study that will be published once completed.

Several other choices could have been made for the control side. We chose the collagen gel alone to directly isolate the role of MSCs on repair outcome using within animal comparisons. Clearly, an empty defect could have been chosen to represent natural repair, especially if the collagen gel without cells might happen to migrate out of the repair site. This approach was taken in our Achilles tendon repair study[13] precisely because of our concern about gel migration. Other possible controls that can be used in future studies include implants containing committed cells (such as fibroblasts or tenocytes).

In this study, grip-to-grip displacement data were used to calculate repair tissue strains. It could be argued that grip-to-grip strain data overestimates tissue strains and underestimates tissue modulus due to nonuniform deformations and potential slippage in the grips. Nonuniform deformations are known to occur along and across tendon during tensile testing. In fact, data in the literature[18,30,31] indicate that the strains in normal tendon and ligament are higher near the bony insertion than in the midsubstance region. Averaging the deformations over the entire tendon length based on the grip-to-grip data typically results in overestimates of soft tissue strain and compliance. Optical surface-strain measuring techniques (such as the video dimension analyzer or VDA) are, thus, more appropriate for measuring the strains within normal tendon and ligament substance. In healing PT, however, the repair region is very compliant, especially in the early phases of healing. Our observations from taped recordings of the failure tests indicate that considerable deformations occurred within the repair tissue. These observations are confirmed by the fact that 100% of the samples tested failed within the isolated repair region. Therefore, the use of grip-to grip displacement data is a valid technique for this healing model.

We conducted the displacement-controlled mechanical tests at a medium strain rate (2% per second) to better monitor the failure sequence. It is well known that the mechanical properties of tendons are minimally rate sensitive.[32–35] For example, ligament stiffness increases only 50% for a 2300-fold increase in rate[34] and tendon modulus increases little or no amount for up to a 100-fold increase in rate.[32,33] Higher strain rates are usually used in normal ligaments and tendons to increase the frequency of midsubstance failures and to minimize insertional and bone avulsion failures.[36–38] With healing tissues, however, failure occurs within the weaker repair region, regardless of the strain rate utilized.

In conclusion, the improvements noted here in the biomechanical properties of the MSC-treated tendons should encourage further research into MSC-mediated tendon repair. Appropriate cell-delivery matrices must still be identified. In the current study, we utilized a nonaligned bovine collagen I matrix to deliver rabbit cells. The benefits of other vehicles such as oriented matrices and type I rabbit collagen should be explored so as to organize the implant earlier and avoid potential rejection problems, respectively. Factors influencing the contraction dynamics of MSC-seeded collagen implants must also be evaluated, including, the roles of cell-seeding density, donor age, and contraction time during incubation *in vitro*. These studies should then be correlated with *in vivo* repair outcome. The knowledge gained from such *in vitro* assays might then benefit those who seek to tissue engineer functional, cell-based implants for various soft and hard tissue injury models.

ACKNOWLEDGMENTS

The authors wish to thank: Roger Ganschow, Scott Hartman, Mark Kurtzman, Jennifer Melzer, Matt Harris, and Juliana Han for their help and contributions to the completion of this study. This study was funded under a NIH sponsored Research Challenge grant to the University of Cincinnati, and NIH grants to Case Western Reserve University.

REFERENCES

1. Caplan, A.I. Mesenchymal stem cells. J. Orthop. Res. **9(5),** 641, 1991.
2. Morrison, S.J., Shah, N.M., and Anderson, D.J. Regulatory mechanisms in stem cell biology. Cell **88,** 287, 1997.
3. Caplan, A.I. The mesengenic process. Clin. Plast. Surg. **21(3),** 429, 1994.
4. Nakahara, H., Dennis, J., Bruder, S., Haynesworth, S., Lennon, D., and Caplan, A. In vitro differentiation of bone and hypertrophic cartilage from periosteal-derived cells. Exp. Cell Res. **195(2),** 492, 1991.
5. Bruder, S.P., Fink, D.J., and Caplan, A.I. Mesenchymal stem cells in bone development, bone repair, and skeletal regeneration therapy. J. Cell. Biochem. **56(3),** 283, 1994.
6. Young, H.E., Ceballos, E.M., Smith, J.C., Mancini, M.L., Wright, R.P., Ragan, B.L., Bushell, I., and Lucas, P.A. Pluripotent mesenchymal stem cells reside within avian connective tissue matrices. In Vitro Cell. Dev. Biol. Anim. **29A(9),** 723, 1993.
7. Young, H.E., Mancini, M.L., Wright, R.P., Smith, J.C., Black, A.C., Jr., Reagan, C.R., and Lucas, P.A. Mesenchymal stem cells reside within the connective tissues of many organs. Dev. Dyn. **202(2),** 137, 1995.
8. Caplan, A., Goto, T., Wakitani, S., Pineda, S., Haynesworth, S., and Goldberg, V. Cell based technologies for cartilage repair. In: Knee Joint Instability. AAOS Symposium Proceedings, Scottsdale, Arizona, 1991.
9. Kojimoto, H., Yasui, N., Goto, T., Matsuda, S., and Shimomura, Y. Bone lengthening in rabbits by callus distraction. The role of periosteum and endosteum. J. Bone Joint Surg. Br. **70(4),** 543, 1988.
10. Wakitani, S., Goto, T., Pineda, S.J., Young, R.G., Mansour, J.M., Caplan, A.I., and Goldberg, V.M. Mesenchymal cell-based repair of large, full-thickness defects of articular cartilage. J. Bone Joint Surg. Am. **76(4),** 579, 1994.
11. Bruder, S., Kraus, K., Goldberg, V., and Kadiyala, S. Critical-sized canine segmental femoral defects are healed by autologous mesenchymal stem cell therapy. Trans. Orthop. Res. Soc. **23,** 147, 1998.
12. Bruder, S., Kurth, A., Shea, M., Hayes, W., and Kadiyala, S. Quantitative parameters of human mesenchymal stem cell-mediated bone regeneration in an orthotopic site. Trans. Orthop. Res. Soc. **22,** 250, 1997.
13. Young, R., Butler, D., Weber, W., Caplan, A., Gordon, S., and Fink, D. Use of mesenchymal stem cells in a collagen matrix for Achilles tendon repair. J. Orthop. Res. **16,** 406, 1998.
14. Young, R.G., Butler, D.L., Weber, W., Gordon, S.L., and Fink, D.J. Mesenchymal stem cell-based repair of rabbit Achilles tendon. Trans. Orthop. Res. Soc. **22,** 249, 1997.
15. Lennon, D., Haynesworth, S., Bruder, S., Jaiswal, N., and Caplan, A. Human and animal mesenchymal progenitor cells from bone marrow: Identification of serum for optimal selection and proliferation. In Vitro Cell. Dev. Biol. Anim. **32,** 602, 1996.
16. Awad, H., Wu, Y, Butler, D., and Boivin, G. Contraction kinetics of cell-seeded collagen gels: Effects of cell-seeding density. In Yoganathan, A. P., ed. Advances in Bioengineering—International Mechanical Engineering Congress and Exposition, Anaheim, ASME, **39,** 29, 1998.
17. Butler, D.L. Kappa Delta Award paper. Anterior cruciate ligament: Its normal response and replacement. J. Orthop. Res. **7(6),** 910, 1989.
18. Butler, D.L., Grood, E.S., Noyes, F.R., Zernicke, R.F., and Brackett, K. Effects of structure and strain measurement technique on the material properties of young human tendons and fascia. J. Biomech. **17(8),** 579, 1984.
19. Butler, D.L., Kay, M.D., and Stouffer, D.C. Comparison of material properties in fascicle-bone units from human patellar tendon and knee ligaments. J. Biomech. **19(6),** 425, 1986.
20. Butler, D.L., Noyes, F.R., and Grood, E.S. Measurement of the mechanical properties of ligaments. In: Feinberg, B.N., and Fleming, D.G., eds. CRC Handbook of Engineering in Medicine and Biology—Section B: Instruments and Measurements, 1. CRC Press, Inc.: West Palm Beach, FL, 1980, pp 279–314.
21. Frank, C., MacFarlane, B., Edwards, P., Rangayyan, R., Liu, Z.Q., Walsh, S., and Bray, R.A. Quantitative analysis of matrix alignment in ligament scars: A comparison of movement versus immobilization in an immature rabbit model. J. Orthop. Res. **9(2),** 219, 1991.
22. Gibbons, J. Nonparametric Statistical Inference. **65,** New York: Marcell Dekker, Inc., 1985, pp. 127–131.
23. Nabeshima, Y., Grood, E.S., Sakurai, A., and Herman, J.H. Uniaxial tension inhibits tendon collagen degradation by collagenase in vitro. J. Orthop. Res. **14(1),** 123, 1996.
24. Beynnon, B.D., Proffer, D., Drez, D.J., Jr., Stankewich, C.J., and Johnson, R.J. Biomechanical assessment of the healing response of the rabbit patellar tendon after removal of its central third. Am. J. Sports Med. **23(4),** 452, 1995.
25. Burks, R.T., Haut, R.C., and Lancaster, R.L. Biomechanical and histological observations of the dog patellar tendon after removal of its central third. Am. J. Sports Med. **18(2),** 146, 1990.
26. Frank, C., Eyre, D., and Shrive, N. Hydroxypyridinium cross-link deficiency in ligament scar. Trans. Orthop. Res. Soc. **19,** 13, 1994.

27. Frank, C., Woo, S.L., Amiel, D., Harwood, F., Gomez, M., and Akeson, W. Medial collateral ligament healing. A multidisciplinary assessment in rabbits. Am. J. Sports Med. **11(6),** 379, 1983.
28. Salehpour, A., Butler, D., Proch, F., Schwartz, H., Feder, S., Doxey, C., and Ratcliffe, A. Dose-dependent response of gamma irradiation on mechanical properties and related biochemical composition of goat bone-patellar tendon-bone allografts. J. Orthop. Res. **13(6),** 898, 1995.
29. Huang, D., Chang, T.R., Aggarwal, A., Lee, R.C., and Ehrlich, H.P. Mechanisms and dynamics of mechanical strengthening in ligament-equivalent fibroblast-populated collagen matrices. Ann. Biomed. Eng. **21,** 289, 1993.
30. Woo, S.L., Gomez, M.A., Seguchi, Y., Endo, C.M., and Akeson, W.H. Measurement of mechanical properties of ligament substance from a bone-ligament-bone preparation. J. Orthop. Res. **1(1),** 22, 1983.
31. Zernicke, R.F., Butler, D.L., Grood, E.S., and Hefzy, M.S. Strain topography of human tendon and fascia. J. Biomech. Eng. **106(2),** 177, 1984.
32. Danto, M.I., and Woo, S.L. The mechanical properties of skeletally mature rabbit anterior cruciate ligament and patellar tendon over a range of strain rates. J. Orthop. Res. **11(1),** 58, 1993.
33. Herrick, W.C., Kingsbury, H.B., and Lou, D.Y. A study of the normal range of strain, strain rate, and stiffness of tendon. J. Biomed. Mater. Res. **12(6),** 877, 1978.
34. Neumann, P., Keller, T.S., Ekstrom, L., and Hansson, T. Effect of strain rate and bone mineral on the structural properties of the human anterior longitudinal ligament. Spine. **19(2),** 205, 1994.
35. Woo, S.L., Peterson, R.H., Ohland, K.J., Sites, T.J., and Danto, M.I. The effects of strain rate on the properties of the medial collateral ligament in skeletally immature and mature rabbits: A biomechanical and histological study. J. Orthop. Res. **8(5),** 712, 1990.
36. Chiba, M., and Komatsu, K. Mechanical responses of the periodontal ligament in the transverse section of the rat mandibular incisor at various velocities of loading in vitro. J. Biomech. **26(4-5),** 561, 1993.
37. Noyes, F.R., DeLucas, J.L., and Torvik, P.J. Biomechanics of anterior cruciate ligament failure: an analysis of strain-rate sensitivity and mechanisms of failure in primates. J. Bone Joint Surg. Am. **56(2),** 236, 1974.
38. Ticker, J.B., Bigliani, L.U., Soslowsky, L.J., Pawluk, R.J., Flatow, E.L., and Mow, V.C. Inferior glenohumeral ligament: Geometric and strain-rate dependent properties. J. Shoulder Elbow Surg. **5(4),** 269, 1996.

Address reprint requests to:
David L. Butler, Ph.D.
Noyes-Giannestras Biomechanics Laboratories
PO Box 210070
University of Cincinnati
Cincinnati, OH 45221-0070

david.butler@uc.edu